

A concurrent multiscale micromorphic molecular dynamics

Shaofan Li and Qi Tong

Citation: *Journal of Applied Physics* **117**, 154303 (2015); doi: 10.1063/1.4916702

View online: <http://dx.doi.org/10.1063/1.4916702>

View Table of Contents: <http://scitation.aip.org/content/aip/journal/jap/117/15?ver=pdfcov>

Published by the [AIP Publishing](#)

Articles you may be interested in

[Hybrid molecular-continuum simulations using smoothed dissipative particle dynamics](#)

J. Chem. Phys. **142**, 044101 (2015); 10.1063/1.4905720

[Multiscale reactive molecular dynamics](#)

J. Chem. Phys. **137**, 22A525 (2012); 10.1063/1.4743958

[A generalized Irving-Kirkwood formula for the calculation of stress in molecular dynamics models](#)

J. Chem. Phys. **137**, 134104 (2012); 10.1063/1.4755946

[Multi-scale analysis of high-speed dynamic friction](#)

J. Appl. Phys. **110**, 093520 (2011); 10.1063/1.3660194

[Rayleigh's instability of Lennard-Jones liquid nanothreads simulated by molecular dynamics](#)

Phys. Fluids **18**, 024103 (2006); 10.1063/1.2173620



A concurrent multiscale micromorphic molecular dynamics

Shaofan Li^{a)} and Qi Tong

Department of Civil and Environmental Engineering, University of California, Berkeley, California 94720, USA

(Received 21 December 2014; accepted 21 March 2015; published online 15 April 2015)

In this work, we have derived a multiscale micromorphic molecular dynamics (MMMD) from first principle to extend the (Andersen)-Parrinello-Rahman molecular dynamics to mesoscale and continuum scale. The multiscale micromorphic molecular dynamics is a con-current three-scale dynamics that couples a fine scale molecular dynamics, a mesoscale micromorphic dynamics, and a macroscale nonlocal particle dynamics together. By choosing proper statistical closure conditions, we have shown that the original Andersen-Parrinello-Rahman molecular dynamics is the homogeneous and equilibrium case of the proposed multiscale micromorphic molecular dynamics. In specific, we have shown that the Andersen-Parrinello-Rahman molecular dynamics can be rigorously formulated and justified from first principle, and its general inhomogeneous case, i.e., the three scale con-current multiscale micromorphic molecular dynamics can take into account of macroscale continuum mechanics boundary condition without the limitation of atomistic boundary condition or periodic boundary conditions. The discovered multiscale scale structure and the corresponding multiscale dynamics reveal a seamless transition from atomistic scale to continuum scale and the intrinsic coupling mechanism among them based on first principle formulation. © 2015 AIP Publishing LLC. [<http://dx.doi.org/10.1063/1.4916702>]

I. INTRODUCTION

In principle, the molecular dynamics (MD) can simulate motions of any macroscale objects that contain as many atoms as possible, provided that we had sufficient computing power. However, a macroscale system has at least more than 10^{23} atoms in order to contain one mole material substance, and it requires more than 10^{15} integration time steps for a MD computation to achieve a second duration of real-time simulation. These pose great challenges to computer speed, CPU time, and data storage. Therefore, the main objective of the current multiscale methods is mainly about how to devise a clever computation algorithm to save computing time and resource rather than discovering new physics through multiscale analysis.

In this work, we would like to look from a different perspective. Suppose that if we had the exascale computing capacity (capable of at least one exaflops 10^{18}s^{-1}), or maybe zettascale computing capacity (capable of at least one zettaflops is 10^{21}s^{-1}), or even yottascale computing capability (capable of at least one yottaflops 10^{24}s^{-1}), which will allow us conducting molecular dynamics simulation of a macroscale system without worrying of computing speed, the question is now: can we use first principle based molecular dynamics simulation to find the motion or deformation of a macroscale system? The answer is NO, and this is why: When we study macroscale physics such as continuum mechanics or continuum thermodynamics, we mainly deal with macroscale statistical variables such as temperature, stress, diffusion concentration or flux, etc., and we seek them as the solution of various macroscale field models or governing equations, and in these models we often use these statistical or

thermodynamics variable based macroscale boundary conditions in solution procedures. For example, the displacement boundary condition that we use in continuum mechanics is not the atom displacement boundary condition, but a statistical condition that characterizes the center of mass of a cluster of atoms on the boundary. As matter of fact, the so-called Lees-Edwards boundary condition is a special case of such macroscale boundary adopted in molecular dynamics, though it is not an arbitrary macroscale displacement boundary condition but a periodic macroscale boundary condition.^{9,12} This is also true for the traction boundary condition in continuum mechanics, and how to enforce the macroscale traction boundary condition in molecular dynamics is still an open question.^{6,7}

If we wish to use first principle based molecular dynamics to find thermodynamics field variable distributions at macroscale, we must know how to apply macroscale boundary conditions to molecular dynamics simulations, or conduct MD simulation with macroscale boundary conditions.^{6,7} We must know how to prescribe and to extrapolate desirable macroscale thermodynamics variable information for a given microscale atomistic simulation, if we wish to relate first principle atomistic simulation to macroscale experiments or measurements. Without this knowledge, we cannot use first principle atomistic simulation in macroscale or even nanoscale engineering applications. In other words, the first principle-based atomistic simulation may not be able to simulate a macroscale physics event without multiscale treatments. The objective of this work is about how to construct a multiscale micromorphic molecular dynamics (MMMD) that is capable of solving macroscale continuum mechanics problems subjected by macroscale boundary conditions.

To set up a solid physical and mathematical foundation, we start the presentation from the equilibrium (Andersen)-

^{a)}Electronic address: shaofan@berkeley.edu

Parrinello-Rahman (APR) molecular dynamics. Thirty some years ago, in his seminal work, Andersen¹ first proposed an isoenthalpic-isobaric ensemble of MD allowing the volume of a cubic lattice cell to vary. Subsequently, Parrinello and Rahman^{25,26} elegantly extended Andersen's formalism to the anisotropic case allowing both the volume and the shape of a MD cell to vary. Since then the APR molecular dynamics has become the standard protocol in molecular dynamics simulations of structural transformation and phase transition.

However, the APR-MD approach has not been thoroughly understood, and this is reflected in both its physical foundation as well as how to extend it beyond the restriction of periodic boundary condition, so that it can bridge across different length scales. Moreover, the APR-MD Lagrangian has been viewed as an *ad hoc* construction, as Parrinello and Rahman once commented in Ref. 26, "... Whether such a Lagrangian is derivable from first principles is a question for further study; its validity can be judged, as of now, by the equations of motion and the statistical ensembles that it generates..."

In recent years, there have been renewed interests in revising APR molecular dynamics, e.g., Refs. 11, 20, 21, and 27, which attempted to extend APR MD to non-equilibrium condition and macroscale simulation. On the other hand, there have been many efforts to formulate multiscale coarse-grained molecular dynamics, e.g., Refs. 2, 13, 16–18, 28, 29, 33, and 36 among many others. In particular, in a series work Chen and Lee²⁻⁵ have discovered that multiscale decomposition of atomistic molecular dynamics will lead to a multiscale micromorphic dynamics. In fact, the micromorphic continuum theory is an intrinsic multiscale theory,⁸ and recently Vernerey *et al.* have found and utilized the multiscale micromorphic structure to construct multiscale homogenization methods.³⁵ In this work, we unveil that there exists a universal multiscale micromorphic microstructure in atomistic molecular dynamics that will allow us to apply macroscale boundary condition to nonequilibrium molecular dynamics. Under general non-equilibrium conditions, APR molecular dynamics can be extended to form a three-scale particle dynamics from microscale to mesoscale, and finally to continuum macroscale mechanics.

The objective of this work is threefold: (1) Partition first principle based molecular dynamics into different scales to achieve a multiscale molecular dynamics that can bridge atomistic scale with continuum scale; (2) develop a nanomechanics paradigm that can solve small scale engineering problems in finite domains by applying macroscale boundary conditions, and (3) simulate phase transition of crystalline materials in an arbitrary local region under non-equilibrium condition.

The paper is organized into five sections. In Sec. II, we shall review and re-interpret the original APR-MD from first principle. In Sec. III, we present the detailed mathematical analysis of the MMMD, including the discussion of multiscale decomposition. In Sec. IV, we shall validate the proposed multiscale micromorphic molecular dynamics by using it to simulate crystal phase transformation. Finally, in Sec. V, we close the presentation by making few comments and remarks.

II. THE ANDERSEN-PARRINELLO-RAHMAN MOLECULAR DYNAMICS

As proposed by Parrinello and Rahman,²⁶ a MD cell is allowed to change its volume and shape, which is described by a 3×3 matrix \mathbf{h} whose column vectors \mathbf{a} , \mathbf{b} , \mathbf{c} are three edges of the cell. The spatial positions of atoms $\mathbf{r}_i, i = 1, 2, \dots, N$ thus can be written in terms of \mathbf{h} and the local coordinates \mathbf{S}_i , which is given as,

$$\mathbf{r}_i = \mathbf{h}(t) \cdot \mathbf{S}_i(t) = \xi_i \mathbf{a} + \eta_i \mathbf{b} + \zeta_i \mathbf{c}, \quad (1)$$

where $i = 1, 2, \dots, N$ is the index of the atoms, and ξ_i, η_i, ζ_i are the projections of the local atom position vector \mathbf{S}_i onto the representative MD cell edge vectors \mathbf{a} , \mathbf{b} , and \mathbf{c} . Note that the local atom coordinates are with respect to the center of mass of the MD cell, which is chosen as the origin of the local coordinate for the representative MD cell.

Remark 1. First since based on definition the center of the cell is the origin of the local coordinate \mathbf{S}_i , and

$$-0.5 \leq \xi_i(t), \eta_i(t), \zeta_i(t) \leq 0.5.$$

Therefore, one may view \mathbf{S}_i as statistical coordinates or variables. Hence, in the rest of the paper, we call the ensemble of local atom positions $\mathbf{S}_i \in \mathcal{B}_S$ as the (equilibrium) statistical configuration of the atomistic system. Second, both the cell size and local coordinates vary with time. Moreover, each MD cell is a set with a fixed (controlled) number of atoms that have fixed mass, but it allows the intrusion of the atoms from the other cells without accepting their membership. Therefore it is neither a fixed control volume (Eulerian), nor a closed control mass (Lagrangian) ensemble.

The original Lagrangian of the Andersen-Parrinello-Rahman molecular dynamics for an isoenthalpic-isobaric (NPH) ensemble is given as,

$$\mathcal{L} = \frac{1}{2} \sum_i m_i \dot{\mathbf{S}}_i \cdot \mathbf{G} \cdot \dot{\mathbf{S}}_i + \frac{1}{2} W \text{Tr}(\dot{\mathbf{h}}^T \dot{\mathbf{h}}) - \frac{1}{2} \sum_i \sum_{j \neq i} V(r_{ij}) - p\Omega, \quad (2)$$

where p is the hydrostatic pressure results from the environment, i.e., the interaction from the atoms outside the cell; $\mathbf{G} = \mathbf{h}^T \cdot \mathbf{h}$; Ω is the current volume of the cell, m_i is the mass of the i -th atom; V is the interatomic potential; $\text{Tr}(\cdot)$ is the trace operator, and W is a quantity with unit of mass \times length², which was not thoroughly justified in the original PR-MD formulation.

The Euler-Lagrangian equations of the PR molecular dynamics^{25,26} are,

$$\frac{d}{dt} \frac{\partial \mathcal{L}}{\partial \dot{\mathbf{h}}} - \frac{\partial \mathcal{L}}{\partial \mathbf{h}} = 0, \quad (3)$$

$$\frac{d}{dt} \frac{\partial \mathcal{L}}{\partial \dot{\mathbf{S}}_i} - \frac{\partial \mathcal{L}}{\partial \mathbf{S}_i} = 0. \quad (4)$$

Following the standard procedure, one may derive the equations of motion for each atom, which are given as follows:

$$\ddot{\mathbf{S}}_i = - \sum_{j \neq i} \left(\frac{V'(r_{ij})}{m_i r_{ij}} \right) (\mathbf{S}_i - \mathbf{S}_j) - \mathbf{G}^{-1} \cdot \dot{\mathbf{G}} \cdot \dot{\mathbf{S}}_i, \quad (5)$$

$$W\ddot{\mathbf{h}} = -(\boldsymbol{\sigma}_{\text{virial}} + p\mathbf{I}) \cdot \mathbf{h}^{-T}\boldsymbol{\Omega}. \quad (6)$$

In Eq. (6), $\boldsymbol{\sigma}_{\text{virial}}$ is the virial stress that is defined as,

$$\boldsymbol{\sigma}_{\text{virial}} = \frac{1}{\Omega} \sum_i \left(-m_i \mathbf{v}_i \otimes \mathbf{v}_i + \frac{1}{2} \sum_{j \neq i} V'(r_{ij}) \left(\frac{\mathbf{r}_{ij} \otimes \mathbf{r}_{ij}}{r_{ij}} \right) \right), \quad (7)$$

where Ω is the volume of the MD cell in the current configuration, and the fine scale velocity \mathbf{v}_i is defined as

$$\mathbf{v}_i = \mathbf{h} \cdot \dot{\mathbf{S}}_i. \quad (8)$$

The original APR-MD is actually a multiscale method, and it couples the mesoscale kinematic variable \mathbf{h} with the microscale variables \mathbf{S}_i . It is probably the earliest attempt to establish multiscale relationship between kinematic variables at different scales. To describe the mesoscale more naturally, Podio-Guidugli²⁷ suggested an alternative formulation of APR-MD based on the concept of nonlinear continuum mechanics.¹⁹ The basic idea is using the well-defined deformation gradient \mathbf{F} to replace the shape tensor of a MD unit cell, \mathbf{h} , which is defined by

$$\mathbf{F} = \mathbf{h}(t) \cdot \mathbf{h}_0^{-1}, \quad (9)$$

where \mathbf{h}_0 is a second order tensor that maps the MD statistical configuration (**S**-configuration) to a continuum referential configuration (**R**-configuration), i.e., $\mathbf{R}_i = \mathbf{h}_0 \mathbf{S}_i$, so that we can use the concept as well as the language of the material-spatial configuration or the Lagrangian-Eulerian description in continuum mechanics in atomistic computations. The relationships among **S**-configuration, **R**-configuration, and **r**-configuration are illustrated in Fig. 1.

In fact, the idea had been suggested in Parrinello and Rahman's original paper,²⁶ and they suggested using $\mathbf{h}_0 = \langle \mathbf{h}(t) \rangle$, which indicated that they had vaguely anticipated a reference configuration thirty years ago. Therefore, in terms of the deformation gradient, we can write,

$$\mathbf{r}_i = \mathbf{h} \cdot \mathbf{S}_i = \mathbf{h} \cdot \mathbf{h}_0^{-1} \cdot \mathbf{R}_i = \mathbf{F}\mathbf{R}_i, \quad \mathbf{R}_i = \mathbf{h}_0 \cdot \mathbf{S}_i, \quad (10)$$

where \mathbf{r}_i are the local atom position (relative to the center of mass) in the current configuration, whereas \mathbf{R}_i are defined as the local atom position in the referential configuration.

Remark 2. In continuum mechanics, the referential configuration is often treated as the initial configuration, which means that the configuration of the system is in its initial state, or it is the frozen state of the system at initial time.

In an atomistic lattice system, it makes sense to specify the initial lattice configuration, i.e., $\mathbf{h}_0 = \mathbf{h}(0)$ but it does not make sense to specify the initial atomic vibration state, because atoms are always oscillating in the lattice, and we cannot freeze atom vibrations if temperature is not zero. The atom vibration only stops when the temperature of the system reaches to absolute zero. Therefore, in both **S**-configuration and **R**-configuration, both $\mathbf{S}_i(t)$ and $\mathbf{R}_i(t)$ are function of time. In fact, one may want to distinguish the time scale as well. For the time t in $\mathbf{S}_i(t)$ and $\mathbf{R}_i(t)$, it is a fine scale time, which has an atomistic time scale; whereas the time variable t in $\mathbf{h}(t)$ has a much larger time scale, i.e., at mesoscale.

By introducing the second Piola-Kirchhoff stress,

$$\mathcal{S} = \det(\mathbf{F})\mathbf{F}^{-1} \cdot \boldsymbol{\sigma}\mathbf{F}^{-T}, \quad (11)$$

where $\boldsymbol{\sigma}$ is the external Cauchy stress, one may set forth an anisotropic Lagrangian as follows:

$$\begin{aligned} \mathcal{L} = & \frac{1}{2} \sum_i m_i \dot{\mathbf{R}}_i \cdot \mathbf{C} \cdot \dot{\mathbf{R}}_i + \frac{1}{2} W \text{Tr}(\mathbf{F}^T \mathbf{F}) \\ & - \frac{1}{2} \sum_i \sum_{j \neq i} V(r_{ij}) + \mathcal{S}^{\text{ext}} : \mathbf{E}\Omega_0, \end{aligned} \quad (12)$$

where $\mathbf{C} = \mathbf{F}^T \mathbf{F}$ is the right Cauchy-Green tensor, $\mathbf{E} = \frac{1}{2}(\mathbf{C} - \mathbf{I})$ is the Green-Lagrangian tensor, \mathcal{S}^{ext} is the externally applied stress, and Ω_0 is the referential volume. Thus, the equation of motion

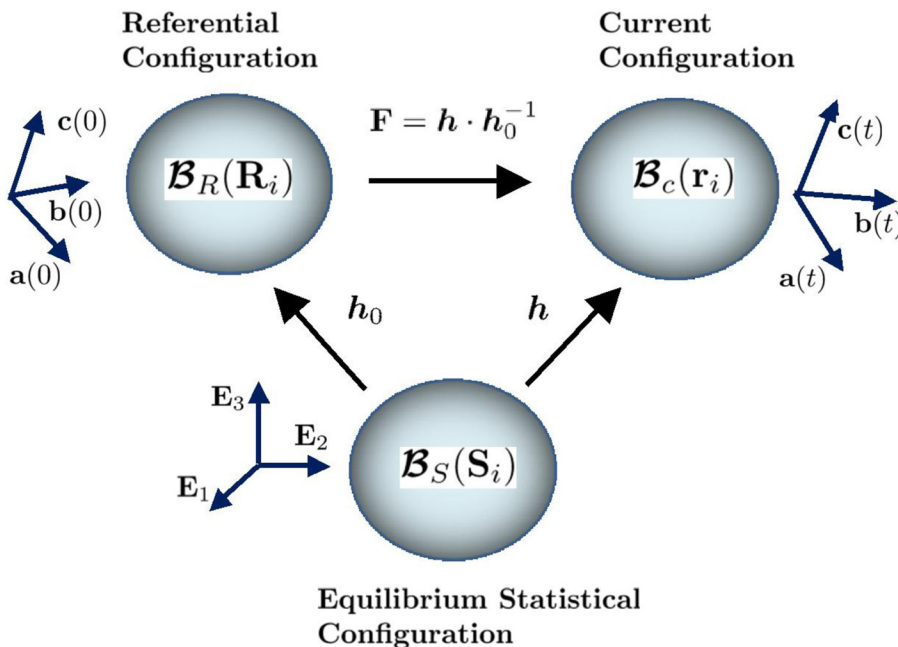


FIG. 1. Differential maps between different lattice configurations of APR-MD, $\mathbf{h} = [\mathbf{a}(t), \mathbf{b}(t), \mathbf{c}(t)]$.

$$\ddot{\mathbf{R}}_i = - \sum_{j \neq i} \left(\frac{V'(r_{ij})}{m_i r_{ij}} \right) (\mathbf{R}_i - \mathbf{R}_j) - \mathbf{C}^{-1} \cdot \dot{\mathbf{C}} \cdot \dot{\mathbf{R}}_i, \quad (13)$$

$$W\ddot{\mathbf{F}} = -\Omega_0 \mathbf{F} (\mathcal{S}_{\text{virial}} - \mathcal{S}^{\text{ext}}), \quad (14)$$

where Ω_0 is the volume of MD cell in the referential configuration, and

$$\begin{aligned} \mathcal{S}_{\text{virial}} &:= \frac{1}{\Omega_0} \sum_i \left(-m_i \dot{\mathbf{R}}_i \otimes \dot{\mathbf{R}}_i + \frac{1}{2} \sum_{j \neq i} \frac{V'(r_{ij})}{r_{ij}} \right. \\ &\quad \left. \times (\mathbf{R}_j - \mathbf{R}_i) \otimes (\mathbf{R}_j - \mathbf{R}_i) \right) \\ &= \frac{1}{\Omega_0} \mathbf{h}_0 \cdot \sum_i \left(-m_i \dot{\mathbf{S}}_i \otimes \dot{\mathbf{S}}_i + \frac{1}{2} \sum_{j \neq i} \frac{V'(r_{ij})}{r_{ij}} \right. \\ &\quad \left. \times (\mathbf{S}_j - \mathbf{S}_i) \otimes (\mathbf{S}_j - \mathbf{S}_i) \right) \cdot \mathbf{h}_0^T. \end{aligned} \quad (15)$$

Remark3. (1) The referential atom position is defined as $\mathbf{R}_i = \mathbf{h}_0 \mathbf{S}_i$, which is not a frozen initial configuration as that of continuum mechanics. It is a referential equilibrium configuration. In the rest of the paper, we refer the configuration $\{\mathbf{S}_i\}$ as the statistical configuration. (2) The anisotropic Lagrangian given in Ref. 27 may have a typo.

In the above derivations, one can see that the approach of using deformation gradient to replace the shape tensor is more convenient to establish an anisotropic multiscale molecular dynamics. However, the modified APR-MD is still limited to a single representative volume element (RVE) cell under equilibrium condition due to its periodic boundary condition and constant stress condition. To overcome this limitation, in Sec. III, we shall discuss a multiscale micromorphic molecular dynamics that is applicable to arbitrary domain with arbitrary macroscale boundary conditions, i.e., it is a multiscale molecular dynamics that supports non-uniform stress field, and it can be subjected to general non-equilibrium conditions. One may note that in molecular dynamics, if spatial distribution of stress is non-uniform, the atomistic system may not be regarded as a mechanical equilibrium state.

III. MMMD

In this section, we shall present a complete mathematical analysis of the multiscale micromorphic molecular dynamics (MMMD), which is an extension of the PR-MD to non-equilibrium state and the molecular systems of finite domain with arbitrary macroscale boundary conditions.

A. Multiscale decomposition

To extend APR molecular dynamics to mesoscale and continuum scale with arbitrary boundary conditions, we first divide the whole atomistic system into many micromorphic cells or local ensembles, and then we consider the following micromorphic multiplicative decomposition for the spatial atomic position in the α th MD cell,

$$\mathbf{r}_i = \mathbf{r}_\alpha + \mathbf{r}_{\alpha i}, \quad \alpha = 1, 2, \dots, M; \quad i = 1, 2, \dots, N_\alpha, \quad (16)$$

where \mathbf{r}_i is the spatial position of the i th atom of the α -cell in the deformed configuration; \mathbf{r}_α is the center of mass of α th unit cell that is defined as,

$$\mathbf{r}_\alpha = \sum_i m_i \mathbf{r}_i / \sum_i m_i. \quad (17)$$

Since $\mathbf{r}_{\alpha i}$ is the relative position vector with respect to the center of the mass of the cell, and by the definition,

$$\sum_i m_i \mathbf{r}_{\alpha i} = 0. \quad (18)$$

In Eq. (16),

$$\mathbf{r}_{\alpha i} = \boldsymbol{\phi}_\alpha \cdot \mathbf{S}_i \quad \text{and} \quad \boldsymbol{\phi}_\alpha := \mathbf{F}_\alpha \cdot \boldsymbol{\chi}_\alpha, \quad (19)$$

where $\boldsymbol{\phi}_\alpha$ is the total deformation tensor of the α th cell, and \mathbf{S}_i is statistical coordinates for the i th atoms inside the α th cell. Here, the second order tensor $\boldsymbol{\chi}_\alpha$ is the shape tensor of α th cell, i.e., $\boldsymbol{\chi}_\alpha = \mathbf{h}_\alpha$. Instead of using Parrinello-Rahman's notation, in this paper we use a different symbol. On the other hand, $\mathbf{F}_\alpha = \mathbf{F}_\alpha(\{\mathbf{r}_\beta\})$ is the coarse scale deformation gradient that is determined by the overall motion of all centers of mass of every cells, and it is completely determined by relative positions or distribution of centers of mass (denoted by $\{\mathbf{r}_\beta\}$) of different cells. In Fig. 2, we show a distribution of centers of mass. \mathbf{F}_α together with $\boldsymbol{\chi}_\alpha$ constitute the total deformation gradient $\boldsymbol{\phi}_\alpha$.

Since the centers of mass are a set of discrete points, it is not a continuous field, and we cannot take spatial derivative on it. In practice, however, we can still determine \mathbf{F}_α by using various numerical techniques. For example, we can employ the approach adopted in reproducing kernel particle method¹⁴ or the state-based peridynamics.³⁰ Let

$$\mathbf{r}_{\alpha\beta} = \mathbf{r}_\beta - \mathbf{r}_\alpha, \quad \mathbf{R}_\alpha := \mathbf{r}_\alpha(0), \quad \text{and} \quad \mathbf{R}_{\alpha\beta} = \mathbf{R}_\beta - \mathbf{R}_\alpha, \quad (20)$$

where the Greek subscripts are indices of the particles that are the center of mass of micromorphic cells.

We can then construct the so-called moment matrix (see Ref. 14),

$$\mathbf{M}_\alpha := \sum_{\beta=1}^{N_h} \omega(|\mathbf{R}_{\alpha\beta}|) \mathbf{R}_\alpha \otimes \mathbf{R}_{\alpha\beta} \Omega_{\beta 0}, \quad (21)$$

where \otimes is the tensor product operator, $\Omega_{\beta 0}$ is the equilibrium volume of the β th cell, N_h is the number of neighboring centers of mass, and $\omega(|\mathbf{R}_{\alpha\beta}|)$ is a localized positive window function. The local deformation gradient tensor can then be constructed as

$$\mathbf{F}_\alpha = \left(\sum_{\beta=1}^{N_h} \omega(|\mathbf{R}_{\alpha\beta}|) \mathbf{r}_{\alpha\beta} \otimes \mathbf{R}_{\alpha\beta} \Omega_{\beta 0} \right) \cdot \mathbf{M}_\alpha^{-1}. \quad (22)$$

Note that $\omega(|\mathbf{R}_{\alpha\beta}|)$ is a localized positive window function, and common choice is the Gaussian function or the cubic spline function. The Gaussian is defined as

$$\omega_h(\mathbf{x}) = \frac{1}{(\pi h^2)^{d/2}} \exp\left(-\frac{\mathbf{x} \cdot \mathbf{x}}{h^2}\right), \quad (23)$$

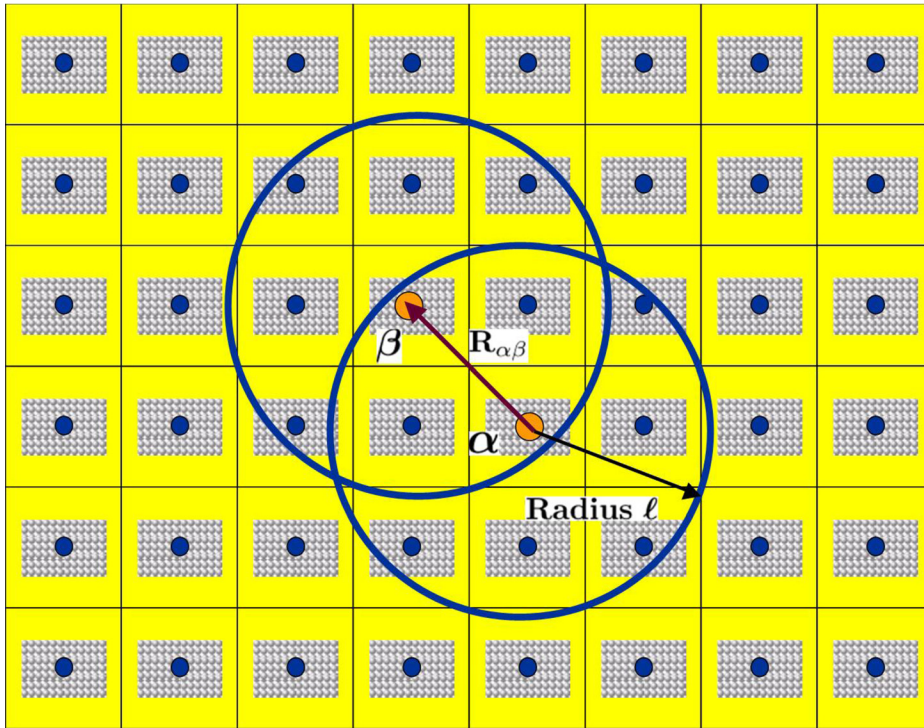


FIG. 2. Local distribution of the centers of mass.

where d is the space dimension and h is the radius of the support. The cubic spline function is often defined as,

$$\omega_h(x) = \frac{A}{h^d} \begin{cases} 1 - \frac{3}{2}x^2 + \frac{3}{4}x^3, & 0 \leq x < 1 \\ \frac{1}{4}(2-x)^3, & 1 \leq x \leq 2 \\ 0, & \text{otherwise} \end{cases} \quad (24)$$

where again d is number of space dimension, h is the radius of the compact support, and

$$A = \begin{cases} 2/3 & 1d \\ 10/(2\pi) & 2d \\ 1/\pi & 3d \end{cases}$$

The initial position of the center of mass, $\mathbf{R}_\alpha = \mathbf{r}_\alpha(0)$, is designated for the center of mass for all MD cells. The definition makes sense because that the time scale in \mathbf{r}_α is a slow scale. For all the atoms in a representative MD cell, say, α th cell, we can define

$$\mathbf{R}_i := \mathbf{R}_\alpha + \mathbf{R}_{\alpha i}, \text{ where } \mathbf{R}_{\alpha i} = \chi_0 \mathbf{S}_i. \quad (25)$$

As mentioned above, this is the initial equilibrium configuration but not the initial ‘‘frozen’’ configuration.

It may be noted that in the above equation, we define \mathbf{R}_i as the total position vector of the i th atom of the α th cell in the referential configuration, whereas in the original PR-MD, i.e., Eq. (10), \mathbf{R}_i is viewed as the relative atom position vector in the representative cell in the referential configuration, which is equivalent to $\mathbf{R}_{\alpha i}$ in Eq. (25). This is because that in PR-MD the position of the center of mass in the representative

cell is the origin of the coordinate $\mathbf{R}_\alpha = 0$, because there is only one MD cell; whereas in MMMD, the position of the center of mass of a micromorphic cell no longer occupies the origin of the global coordinate, i.e., $\mathbf{R}_\alpha \neq 0$, because there are many MD cells.

By doing so, we can describe the equilibrium referential configuration \mathcal{B}_R . One can see that this definition is consistent with kinematic assumption,

$$\mathbf{r}_i = \mathbf{r}_\alpha + \mathbf{r}_{\alpha i} = \mathbf{r}_\alpha + \mathbf{F}_\alpha \cdot \chi_\alpha \cdot \mathbf{S}_i. \quad (26)$$

Based on Eq. (26), we may define an intermediate referential configuration,

$$\mathcal{R}_i = \mathbf{R}_\alpha + \mathcal{R}_{\alpha i} = \mathbf{R}_\alpha + \chi_\alpha \cdot \mathbf{S}_i, \quad (27)$$

so that the coarse scale deformation gradient becomes the deformation gradient in the rigorous sense of continuum mechanics.

To summarize, in the proposed multiscale micromorphic molecular dynamics, there are four configurations: the statistical configuration \mathcal{B}_S , the equilibrium referential configuration \mathcal{B}_R , the intermediate configuration \mathcal{B}_I , and the current configuration \mathcal{B}_C . In Fig. 3, we show the deformation maps that connect these configuration spaces.

Remark 4. (1) First, each MD cell is a supercell of the underline lattice, or atom cluster, and it is not the smallest unit cell. More precisely, it is set of atoms in a local ensemble rather than in a local fixed spatial region or volume.

(2) It may be noted that in the modified PR-MD,²⁷ $\mathbf{F} := \mathbf{h} \cdot \mathbf{h}_0^{-1}$ with $\mathbf{h}_0 := \langle \mathbf{h}(t) \rangle$, which is a mesoscale variable, i.e., it is at the same scale as the mesoscale variable $\mathbf{h}(t)$. A shortcoming for such approach is that the definition of \mathbf{h}_0 is posterior. Whereas in MMMD, \mathbf{F}_α are solely determined by the

relative positives of set of centers of mass for MD cells, therefore, they are coarse scale variables.

(3) In the modified PR-MD,²⁷ the deformation gradient \mathbf{F} is essentially a mesoscale map $\mathbf{R}_i \rightarrow \mathbf{r}_i$; whereas in MMMD, the deformation gradient \mathbf{F}_α is a coarse scale deformation gradient depending on the positions of centers of mass of different MD cells in both the current configuration as well as the referential configuration, i.e., $\mathbf{R}_\alpha \rightarrow \mathbf{r}_\alpha$.

Note that $\mathbf{r}_\alpha(t)$ are independent from fine scale statistical variables, therefore, it makes sense to specify its initial value $\mathbf{r}_\alpha(0)$, whereas in the fine scale $\mathbf{S}_i(0)$ may not be used as a reference value. It may be tempting to define

$$\mathbf{R}_{\alpha i} := \mathbf{R}_i - \mathbf{R}_\alpha = \mathbf{r}_{\alpha i}(0).$$

However, such definition would be meaningless, because $\mathbf{r}_{\alpha i}(t)$ are functions of atomic time scale, which really do not have a special time instance that can be used as the initial mark of the beginning that is suitable for every oscillating atoms. In fact, $\mathbf{R}_{\alpha i}(t) = \chi_{\alpha 0} \mathbf{S}_i(t)$, and it oscillates all the time.

In the proposed multiscale method, we have introduced four different configurations in a representative cell α : (1) The spatial configuration, i.e., the \mathbf{r} -configuration, in which $\mathbf{r}_i \in \Omega_\alpha$; (2) the intermediate equilibrium configuration, i.e., \mathcal{R} -configuration, (3) the referential equilibrium configuration, i.e., the \mathbf{R} -configuration, in which $\mathbf{R}_i \in \Omega_{\alpha 0}$, and the statistical configuration \mathbf{S}_i . It may be noted that in the configuration spaces $\mathcal{B}_I, \mathcal{B}_R$, the centers of mass coordinates are the same, i.e., \mathbf{R}_α , whereas for the statistical configuration space \mathcal{B}_S , it varies cell by cell, and the coordinates of the center of mass for each cell are zero.

Even though the referential configuration is not essential in the fine scale calculation, but its information is needed in the coarse scale computation. To make the deformation decomposition at each scale clear, we consider the following atomic position decomposition:

$$\mathbf{r}_i = \mathbf{r}_\alpha + \mathbf{r}_{\alpha i} \Rightarrow \mathbf{r}_i = \mathbf{r}_\alpha + \mathbf{F}_\alpha \cdot \mathcal{R}_{\alpha i} = \mathbf{r}_\alpha + \mathbf{F}_\alpha \cdot \chi_\alpha \cdot \mathbf{S}_i, \tag{28}$$

where

$$\mathcal{R}_{\alpha i} = \chi_\alpha \cdot \mathbf{S}_i.$$

Subsequently, we can decompose or separate the atomistic displacement into three different scales,

$$\begin{aligned} \bar{\mathbf{u}}_i &= (\mathbf{r}_\alpha - \mathbf{R}_\alpha); \\ \tilde{\mathbf{u}}_i &= (\mathbf{F}_\alpha \cdot \chi_\alpha - \chi_\alpha) \mathbf{S}_i; \\ \mathbf{u}'_i &= (\chi_\alpha - \chi_{\alpha 0}) \mathbf{S}_i, \end{aligned} \tag{29}$$

where $\bar{\mathbf{u}}_i, \tilde{\mathbf{u}}_i, \mathbf{u}'_i$ denote macroscale, mesoscale, and micro-scale displacements. Apparently, three of them together constitute the total displacement \mathbf{u}_i , which can be expressed as,

$$\mathbf{u}_i = \bar{\mathbf{u}}_i + \tilde{\mathbf{u}}_i + \mathbf{u}'_i = \mathbf{r}_i - \mathbf{R}_i. \tag{30}$$

Considering the length scale of the displacements as $\|\bar{\mathbf{u}}_i\| = l_r$, $\|\tilde{\mathbf{u}}_i\| = l_c$ and $\|\mathbf{u}'_i\| = l_a$, we have the relationship

$$l_a \ll l_c \ll l_r, \tag{31}$$

for the associated time scales t_r, t_c , and t_a , we also have

$$t_a \ll t_c \ll t_r. \tag{32}$$

In spatial scale decomposition, we select three independent kinematic variables, $\{\mathbf{S}_i, \chi_\alpha, \text{ and } \mathbf{r}_\alpha\}$ corresponding to three different spatial scales. The novelty of the above multiscale decomposition is the following **Micromorphic Multiscale Decomposition**,

$$\phi_\alpha = \mathbf{F}_\alpha \cdot \chi_\alpha, \tag{33}$$

which is a multiplicative decomposition. Fig. 3 schematically depicts the deformation map and scale decomposition of the atomistic system at different scales. The total deformation gradient ϕ_α consists of a macro deformation \mathbf{F}_α and micromorphic (meso) deformation χ_α . The mapping of \mathbf{F}_α may be referred to as the **Long-range order**, whereas the mapping of χ_α may be referred to as the **Short-range order**.

Remark 5. (1) The main objective of MMMD is to extend the equilibrium PR-MD to the case of non-equilibrium molecular dynamics processes. The key approach adopted here is the local equilibrium assumption (LEA), which means that the local equilibrium may be attained in a local micromorphic cell. (2) The micromorphic cell division is a Lagrangian division, meaning that each cell is a control atom number (N) cell, or it is a local $N\sigma H$ or a local $N SH$ ensemble, but not a control volume (Eulerian) cell, which is also different from Lagrangian control volume ensemble such as a local NVT ensemble cell.^{15,16}

The MMMD formulation is basically a multiscale Lagrangian repartition of the original first principle Lagrangian, and the added additional topological constraints will not affect the original first principle Lagrangian in principle. It essentially serves as statistical guidance in MD simulations. That is, it is a device to extrapolate and manifest statistical meanings or contents of first principle MD simulation. Therefore, we allow cell overlap, penetration, as well as having gaps between them. If that is what really happened in the original atomistic system. This philosophy is illustrated in Fig. 4.

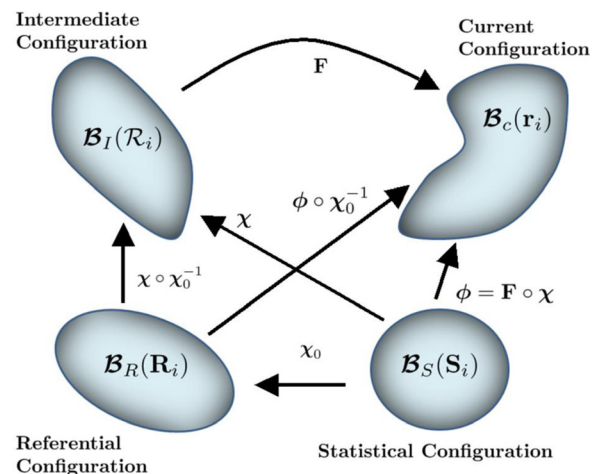


FIG. 3. Deformation maps among different kinematic configurations of MMMD.

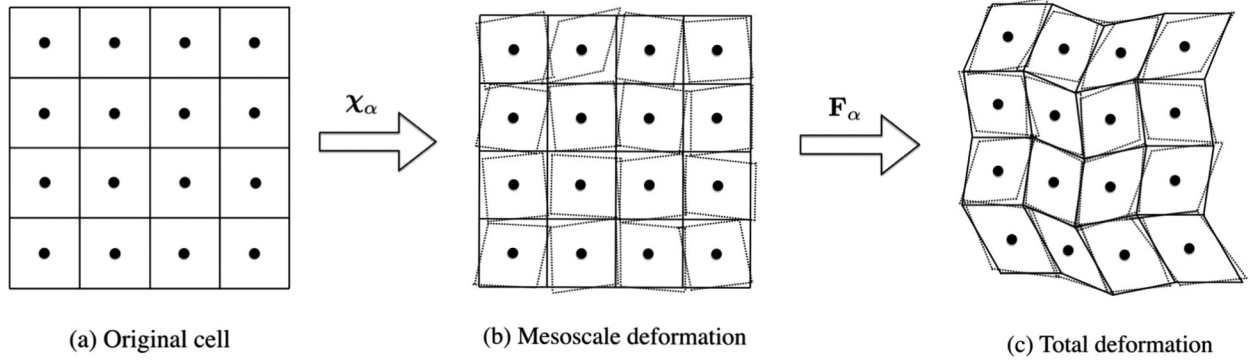


FIG. 4. Cell-level deformation: (a) The original undeformed system which is divided into several unit cells. The atomic positions are given by \mathbf{R}_i . The solid circles represent the centers of mass. (b) The configuration undergoes macroscale deformation \mathbf{F}_α . Notice that the cells are connected to each other without gaps or overlaps in the framework of continuity, and this deformation is restrained by the relative positions of centers of mass of different cells. (c) The cells (dashed parallelograms) further undergo microscale deformation χ_α around their own center of mass separately without connection. This is because that the assumption of continuity is no longer valid in the fine scale.

In passing, we note that the continuum compatibility condition is a macroscale condition, and at both microscale and mesoscale this condition is not necessarily satisfied. For crystalline solids, this may be linked to the defect states or quasi-crystal states.

B. Statistical conditions

Before constructing the governing equations for MMMD, we would like to revisit the statistical conditions implied in APR-MD, and provide some explanations or interpretations for them. Consider the kinetic energy of the α th cell

$$\begin{aligned}
 K_\alpha &= \frac{1}{2} \sum_i m_i \dot{\mathbf{r}}_i \cdot \dot{\mathbf{r}}_i = \frac{1}{2} \sum_i m_i (\dot{\mathbf{r}}_\alpha + \dot{\phi}_\alpha \cdot \mathbf{S}_i + \phi_\alpha \cdot \dot{\mathbf{S}}_i) \cdot (\dot{\mathbf{r}}_\alpha + \dot{\phi}_\alpha \cdot \mathbf{S}_i + \phi_\alpha \cdot \dot{\mathbf{S}}_i) \\
 &= \underbrace{\frac{M_\alpha}{2} \dot{\mathbf{r}}_\alpha \cdot \dot{\mathbf{r}}_\alpha}_{K_1} + \underbrace{\frac{1}{2} \dot{\phi}_\alpha^T \phi_\alpha \sum_i m_i \mathbf{S}_i \otimes \mathbf{S}_i}_{K_2} + \underbrace{\frac{1}{2} \sum_i m_i \dot{\mathbf{S}}_i \cdot \mathbf{C} \cdot \dot{\mathbf{S}}_i}_{K_3} + \underbrace{\frac{1}{2} \dot{\phi}_\alpha^T \phi_\alpha \sum_i m_i \mathbf{S}_i \otimes \dot{\mathbf{S}}_i + \frac{1}{2} \phi_\alpha^T \dot{\phi}_\alpha \sum_i m_i \dot{\mathbf{S}}_i \otimes \mathbf{S}_i}_{K_4}, \quad (34)
 \end{aligned}$$

where $M_\alpha = \sum_i m_i$ is the mass of the α th cell, and $\mathbf{C} = \phi_\alpha^T \phi_\alpha$. Introduce the following statistical assumption:

$$\begin{aligned}
 \mathbf{J}_\alpha^S &= \sum_i m_i \mathbf{S}_i \otimes \mathbf{S}_i = \sum_i m_i \chi_{\alpha 0}^{-1} \cdot \mathbf{R}_{\alpha i} \otimes \mathbf{R}_{\alpha i} \cdot \chi_{\alpha 0}^{-T} \\
 &= \chi_{\alpha 0}^{-1} \cdot \mathbf{J}_\alpha \cdot \chi_{\alpha 0}^{-T} = \text{constant tensor}. \quad (35)
 \end{aligned}$$

Here, we assume that \mathbf{J}_α^S is a spherical and constant second order tensor,²⁷ and this fact stems from the fundamental assumption of ergodicity in molecular dynamics systems, i.e., the space and time are statistical homogeneous in statistical configuration. Note that \mathbf{J}_α^S is a quantity in statistical configuration, $\mathbf{B}_S(\mathbf{S}_i)$, and it is not from the real physical configuration. In Eq. (35), we have defined,

$$\mathbf{J}_\alpha = \sum_i m_i \mathbf{R}_{\alpha i} \otimes \mathbf{R}_{\alpha i} = \chi_{\alpha 0} \mathbf{J}_\alpha^S \chi_{\alpha 0}^T \quad (36)$$

as the referential Euler's inertia tensor of the cell, which is anisotropic and is dependent on the shape and size of the micromorphic cell, because \mathbf{J}_α is the pushforward of \mathbf{J}_α^S ,¹⁹ and here $\chi_{\alpha 0} = \chi(0)$ is a constant second tensor, i.e., the geometric shape tensor of the original cell.

If we choose \mathbf{E}_I as principal axes, we can have a simple expression of \mathbf{J}_α^S ,

$$\mathbf{J}_\alpha^S = J_{11}^S \mathbf{E}_1 \otimes \mathbf{E}_1 + J_{22}^S \mathbf{E}_2 \otimes \mathbf{E}_2 + J_{33}^S \mathbf{E}_3 \otimes \mathbf{E}_3. \quad (37)$$

Since \mathbf{J}_α^S is spherical, we may write $J_{11}^S = J_{22}^S = J_{33}^S = W_\alpha$. Now it becomes clear that the quantity W used in the original PR-MD is related to the component of Euler's inertia tensor. Therefore, naturally, the second term of kinetic energy becomes

$$K_2 = \frac{1}{2} W_\alpha \text{Tr}(\dot{\phi}_\alpha^T \dot{\phi}_\alpha). \quad (38)$$

We call expression (35) as the **First statistical condition** of APR-MD.

Next we consider the fourth term of the kinetic energy K_4 . Since \mathbf{S}_i is labeled as statistical variables, we can define their tensorial autocorrelation function as follows:

$$\text{AC}(\tau) = \langle \mathbf{S}_i(t) \otimes \mathbf{S}_i(t + \tau) \rangle := \sum_i m_i \mathbf{S}_i(t) \otimes \mathbf{S}_i(t + \tau). \quad (39)$$

If we assume that the autocorrelation tensor is an isotropic tensor or a spherical tensor, i.e.,

$$\begin{aligned}
 \text{AC}(\tau) &= \sum_i m_i \mathbf{S}_i(t) \otimes \mathbf{S}_i(t + \tau) \\
 &= \left(\sum_i m_i s_i(t) s_i(t + \tau) \right) \mathbf{E}_I \otimes \mathbf{E}_I,
 \end{aligned}$$

where \mathbf{E}_I , $I = 1, 2, 3$ are the basis vectors for a Cartesian coordinate. We can prove that the autocorrelation tensor is an even function of τ , if we assume that the statistical tensor $\sum_i \mathbf{S}_i \otimes \mathbf{S}_i$ is spherical. This implies that the time derivative of the autocorrelation function tensor at the origin of $\tau = 0$ is zero. Hence,

$$\frac{d}{d\tau} \mathbf{AC}|_{\tau=0} = \sum_i m_i \mathbf{S}_i(t) \otimes \dot{\mathbf{S}}_i(t) = 0, \quad (40)$$

and similarly,

$$\sum_i m_i \dot{\mathbf{S}}_i(t) \otimes \mathbf{S}_i(t) = 0. \quad (41)$$

We refer the conditions (40) and (41) as the **Second statistical condition**, which gives $K_4 = 0$. In fact, the First statistical condition implies that

$$\frac{d}{dt} \mathbf{J}_\alpha^S = \sum_i m_i \dot{\mathbf{S}}_i(t) \otimes \mathbf{S}_i(t) + \sum_i m_i \mathbf{S}_i(t) \otimes \dot{\mathbf{S}}_i(t) = 0,$$

which is a weaker condition than Eqs. (40) and (41).

Remark 6. Mathematically, conditions (40) and (41) ensure that the variables $\boldsymbol{\chi}_\alpha$ and \mathbf{S}_i are independent. Since the physical meaning of $\boldsymbol{\chi}_\alpha$ is the shape and size of the α th cell, one can see from the Parrinello-Rahman decomposition

$$\mathcal{R}_{\alpha i} = \boldsymbol{\chi}_\alpha \cdot \mathbf{S}_i,$$

that if the length of \mathbf{S}_i is not fixed, $\boldsymbol{\chi}_\alpha$ may not represent the shape tensor of the α th cell. Therefore, we must have the constraint condition,

$$\sum_i \mathbf{S}_i \cdot \mathbf{S}_i = \text{const}, \quad (42)$$

which is a weaker condition than conditions (40) and (41).

By utilizing above statistical conditions, we can conveniently write down the Lagrangian of the atomic system as,

$$\begin{aligned} \mathcal{L}_m = & \frac{1}{2} \sum_\beta M_\beta \dot{\mathbf{r}}_\beta \cdot \dot{\mathbf{r}}_\beta + \frac{1}{2} \sum_\beta \mathbf{J}_\beta^S : \left(\dot{\boldsymbol{\phi}}_\beta^T \dot{\boldsymbol{\phi}}_\beta \right) \\ & + \frac{1}{2} \sum_\beta \sum_i m_i \dot{\mathbf{S}}_i \cdot \mathbf{C}_\beta \cdot \dot{\mathbf{S}}_i \\ & - \frac{1}{2} \sum_\beta \sum_\gamma \sum_{i \in \beta, j \in \gamma} V(r_{ij}) + \sum_\beta \sum_{i \in \beta} \mathbf{b}_i \cdot \mathbf{r}_i, \end{aligned} \quad (43)$$

where β, γ are cell indices, and the abbreviation $i \in \beta$ means that it is the i th atom in the β th cell. $\mathbf{C}_\beta := \boldsymbol{\phi}_\beta^T \boldsymbol{\phi}_\beta$ is the micro right Cauchy-Green tensor for total deformation.

In the following presentation, we choose three independent field variables, \mathbf{r}_α , $\boldsymbol{\phi}_\alpha$, and \mathbf{S}_i representing kinematic variables for three different scales, instead of the set of original variables $\mathbf{r}_\alpha, \boldsymbol{\chi}_\alpha, \mathbf{S}_i$, which may be equivalent each other. Thus, $\mathcal{L}_m = \mathcal{L}_m(\mathbf{r}_\alpha, \boldsymbol{\phi}_\alpha, \mathbf{S}_i)$. The equations of motion are stated as

$$\frac{d}{dt} \frac{\partial \mathcal{L}_m}{\partial \dot{\mathbf{r}}_\alpha} - \frac{\partial \mathcal{L}_m}{\partial \mathbf{r}_\alpha} = 0, \quad (44)$$

$$\frac{d}{dt} \frac{\partial \mathcal{L}_m}{\partial \dot{\boldsymbol{\phi}}_\alpha} - \frac{\partial \mathcal{L}_m}{\partial \boldsymbol{\phi}_\alpha} = 0, \quad (45)$$

$$\frac{d}{dt} \frac{\partial \mathcal{L}_m}{\partial \dot{\mathbf{S}}_i} - \frac{\partial \mathcal{L}_m}{\partial \mathbf{S}_i} = 0. \quad (46)$$

In Subsections III C–III F, we shall present detailed derivations of these equations.

C. Coarse scale dynamic equation

We start by deriving some useful relations that are needed in the subsequent derivations. Since we know that

$$\mathbf{F}_\beta = \mathbf{F}_\beta(\{\mathbf{r}_\alpha\}) \quad (47)$$

and

$$\dot{\mathbf{F}}_\beta = \dot{\mathbf{F}}_\beta(\{\mathbf{r}_\alpha\}, \{\dot{\mathbf{r}}_\alpha\}), \quad (48)$$

we then have

$$\ddot{\mathbf{F}}_\beta = \sum_\alpha \frac{\partial \mathbf{F}_\beta}{\partial \mathbf{r}_\alpha} \ddot{\mathbf{r}}_\alpha, \quad (49)$$

which leads to the relation,

$$\frac{\partial \dot{\mathbf{F}}_\beta}{\partial \dot{\mathbf{r}}_\alpha} = \frac{\partial \mathbf{F}_\beta}{\partial \mathbf{r}_\alpha} \quad (50)$$

and

$$\ddot{\mathbf{F}}_\beta = \sum_\alpha \left(\frac{d}{dt} \left(\frac{\partial \mathbf{F}_\beta}{\partial \mathbf{r}_\alpha} \right) \dot{\mathbf{r}}_\alpha + \frac{\partial \mathbf{F}_\beta}{\partial \mathbf{r}_\alpha} \ddot{\mathbf{r}}_\alpha \right). \quad (51)$$

On the other hand, we may derive,

$$\ddot{\mathbf{F}}_\beta = \sum_\alpha \left(\frac{\partial \dot{\mathbf{F}}_\beta}{\partial \dot{\mathbf{r}}_\alpha} \ddot{\mathbf{r}}_\alpha + \frac{\partial \mathbf{F}_\beta}{\partial \dot{\mathbf{r}}_\alpha} \dot{\mathbf{r}}_\alpha \right). \quad (52)$$

Comparing Eqs. (51) and (52) and utilizing Eq. (50), we obtain

$$\frac{d}{dt} \left(\frac{\partial \mathbf{F}_\beta}{\partial \mathbf{r}_\alpha} \right) = \frac{\partial \dot{\mathbf{F}}_\beta}{\partial \mathbf{r}_\alpha}. \quad (53)$$

Furthermore, since

$$\dot{\boldsymbol{\phi}}_\beta = \dot{\mathbf{F}}_\beta \boldsymbol{\chi}_\beta + \mathbf{F}_\beta \cdot \dot{\boldsymbol{\chi}}_\beta, \quad (54)$$

we can find that

$$\frac{\partial \dot{\boldsymbol{\phi}}_\beta}{\partial \dot{\mathbf{r}}_\alpha} = \frac{\partial \dot{\mathbf{F}}_\beta}{\partial \dot{\mathbf{r}}_\alpha} \boldsymbol{\chi}_\beta = \frac{\partial \mathbf{F}_\beta}{\partial \mathbf{r}_\alpha} \boldsymbol{\chi}_\beta = \frac{\partial \boldsymbol{\phi}_\beta}{\partial \mathbf{r}_\alpha}. \quad (55)$$

By virtue of Eqs. (53)–(55), we have

$$\begin{aligned} \frac{\partial \dot{\boldsymbol{\phi}}_\beta}{\partial \mathbf{r}_\alpha} &= \frac{\partial \dot{\mathbf{F}}_\beta}{\partial \mathbf{r}_\alpha} \boldsymbol{\chi}_\beta + \frac{\partial \mathbf{F}_\beta}{\partial \mathbf{r}_\alpha} \dot{\boldsymbol{\chi}}_\beta = \frac{\partial \mathbf{F}_\beta}{\partial \mathbf{r}_\alpha} \dot{\boldsymbol{\chi}}_\beta + \frac{d}{dt} \left(\frac{\partial \mathbf{F}_\beta}{\partial \mathbf{r}_\alpha} \right) \boldsymbol{\chi}_\beta \\ &= \frac{d}{dt} \left(\frac{\partial \boldsymbol{\phi}_\beta}{\partial \mathbf{r}_\alpha} \right) = \frac{d}{dt} \left(\frac{\partial \dot{\boldsymbol{\phi}}_\beta}{\partial \dot{\mathbf{r}}_\alpha} \right). \end{aligned} \quad (56)$$

The relations (55)–(56) are needed in the subsequent derivation.

Reconsidering the Lagrangian equation at the coarse scale Eq. (44) and utilizing the above relation, we have

$$\mathcal{P}_\alpha^{int} := \frac{1}{\Omega_{\alpha 0}} \sum_{i \in \alpha} \left(-\phi_\alpha m_i \dot{\mathbf{S}}_i \otimes \dot{\mathbf{S}}_i + \frac{1}{2} \sum_{j \in \alpha, j \neq i} \mathbf{f}_{ij} \otimes \mathbf{S}_{ij} \right), \quad (67)$$

$$\mathcal{P}_\alpha^{ext} = \frac{1}{\Omega_{\alpha 0}} \sum_{\beta \neq \alpha} \sum_{i \in \alpha, j \in \beta} \mathbf{f}_{ij} \otimes \mathbf{S}_i \quad (68)$$

where $\Omega_{\alpha 0}$ is the volume of α th cell in the reference configuration, i.e., \mathbf{R} -configuration.

Remark 7. (1) There is no 1/2 factor in Eq. (68). This is because $i \in \alpha$ but $j \in \beta$, and $\alpha \neq \beta$;

(2) If we define,

$$\begin{aligned} \sigma_\alpha^{ext} &= \frac{1}{\Omega_\alpha} \sum_{\beta \neq \alpha} \sum_{i \in \alpha, j \in \beta} \mathbf{f}_{ij} \otimes \mathbf{r}_{xi} \\ &= \frac{1}{\det(\phi_\alpha) \Omega_{\alpha 0}} \sum_{\beta \neq \alpha} \sum_{i \in \alpha, j \in \beta} \mathbf{f}_{ij} \otimes \mathbf{S}_i \cdot \phi_\alpha^T, \end{aligned} \quad (69)$$

where Ω_α is the volume of the α th cell in spatial configuration, i.e., \mathbf{B}_c -configuration, \mathcal{P}_α^{ext} can then be expressed by the external Cauchy stress as

$$\mathcal{P}_\alpha^{ext} = \det(\phi_\alpha) \sigma_\alpha^{ext} \cdot \phi_\alpha^{-T}. \quad (70)$$

With above definitions of stresses, we can recast the mesoscale dynamics equations as

$$\ddot{\phi}_\alpha \cdot \mathbf{J}_\alpha^S = -(\mathcal{P}_\alpha^{int} - \mathcal{P}_\alpha^{ext}) \Omega_{\alpha 0} + \mathcal{M}_\alpha, \quad (71)$$

where \mathcal{P}_α^{int} is given by Eq. (67), and \mathcal{P}_α^{ext} is given by Eq. (68) or (70), $\mathcal{M}_\alpha = \sum_{i \in \alpha} \mathbf{b}_i \otimes \mathbf{S}_i$ is the mesoscale external couple. Note that Eqs. (67) and (68) are insightful, because they resolve one of the outstanding debates on the definition of the virial stress. Equation (67) is basically the mathematical definition of the virial stress, e.g., Refs. 10 and 32. However, Zhou³⁷ argued that the kinetic energy part should be dropped out in the stress calculation, even though many disagreed, e.g., Refs. 24 and 31. We now see from Eqs. (67) and (68) that if the stress is internally generated, the definition of the virial stress is the original definition of the virial stress; but if the stress is an external stress, then the kinetic energy part should drop out from its expression. This is because that the present formulation of the multiscale micromorphic molecular dynamics is an adiabatic formulation, which does not consider the heat exchange among the cells.

E. Microscale dynamic equations

For simplicity, we re-index the multiscale Lagrangian as

$$\begin{aligned} \mathcal{L}_m &= \sum_\alpha \frac{M_\alpha}{2} \dot{\mathbf{r}}_\alpha \cdot \dot{\mathbf{r}}_\alpha + \frac{1}{2} \sum_\alpha \mathbf{J}_\alpha : \left(\dot{\phi}_\alpha^T \dot{\phi}_\alpha \right) \\ &+ \frac{1}{2} \sum_\alpha \sum_i m_i \dot{\mathbf{S}}_i \cdot \mathbf{C}_\alpha \cdot \dot{\mathbf{S}}_i - \frac{1}{2} \sum_\alpha \sum_\beta \sum_{i \neq j} V(r_{ij}) \\ &+ \sum_\alpha \sum_{i \in \alpha} \mathbf{b}_i \cdot \phi_\alpha \mathbf{S}_i + \sum_\alpha S_{\alpha 0} \bar{\mathbf{t}}_{\alpha 0} \cdot \mathbf{r}_\alpha - \sum_\alpha \Omega_{\alpha 0} \bar{\mathbf{b}}_{\alpha 0} \cdot \mathbf{r}_\alpha, \end{aligned} \quad (72)$$

where the microscale variable \mathbf{S}_i , $i \in \alpha$ and \mathbf{S}_j , $j \in \beta$. In calculations, there are two distinct cases

$$(a) \alpha = \beta, \quad \mathbf{r}_{ij} = \phi_\alpha \cdot \mathbf{S}_{ij}, \quad \frac{\partial r_{ij}}{\partial \mathbf{S}_i} = -\frac{\mathbf{r}_{ij}}{r_{ij}} \cdot \phi_\alpha = -\frac{\mathbf{C}_\alpha \cdot \mathbf{S}_{ij}}{r_{ij}}, \quad (73)$$

$$(b) \alpha \neq \beta: \quad \mathbf{r}_{ij} = \mathbf{r}_{\alpha\beta} + (\phi_\beta \cdot \mathbf{S}_j - \phi_\alpha \cdot \mathbf{S}_i), \quad \frac{\partial r_{ij}}{\partial \mathbf{S}_i} = -\frac{\mathbf{r}_{ij}}{r_{ij}} \cdot \phi_\alpha. \quad (74)$$

Evaluating the fine scale Lagrangian equation for $i \in \alpha$,

$$\frac{d}{dt} \frac{\partial \mathcal{L}_m}{\partial \dot{\mathbf{S}}_i} - \frac{\partial \mathcal{L}_m}{\partial \mathbf{S}_i} = 0, \quad i \in \alpha,$$

we have

$$\frac{d}{dt} \frac{\partial \mathcal{L}_m}{\partial \dot{\mathbf{S}}_i} = m_i (\mathbf{C}_\alpha \ddot{\mathbf{S}}_i + \dot{\mathbf{C}}_\alpha \cdot \dot{\mathbf{S}}_i)$$

and

$$(a) \alpha = \beta: \quad \frac{\partial \mathcal{L}_m}{\partial \mathbf{S}_i} = \sum_{j \neq i} \left(\frac{V'(r_{ij})}{r_{ij}} \mathbf{C}_\alpha \cdot \mathbf{S}_{ij} \right), \quad (75)$$

$$(b) \alpha \neq \beta: \quad \frac{\partial \mathcal{L}_m}{\partial \mathbf{S}_i} = \sum_{\alpha \neq \beta} \sum_{j \neq i} \left(\frac{V'(r_{ij})}{r_{ij}} \phi_\alpha^T \cdot \mathbf{r}_{ij} \right),$$

where $\mathbf{r}_{ij} = \mathbf{r}_{\alpha\beta} + \phi_\beta \cdot \mathbf{S}_j - \phi_\alpha \cdot \mathbf{S}_i$. Note that the factor 1/2 vanishes in case (a) because each atom pair is summed twice.

Finally, we can express the fine scale dynamics equations as,

$$(a) \alpha = \beta: \quad \ddot{\mathbf{S}}_i = \sum_{j \neq i} \left(\frac{V'(r_{ij})}{r_{ij}} \mathbf{S}_{ij} \right) - \mathbf{C}_\alpha^{-1} \dot{\mathbf{C}}_\alpha \cdot \dot{\mathbf{S}}_i, \quad (76)$$

$$\begin{aligned} (b) \alpha \neq \beta: \quad \ddot{\mathbf{S}}_i &= \phi_\alpha^{-1} \sum_{\alpha \neq \beta} \sum_{i \neq j} \\ &\times \left(\frac{V'(r_{ij})}{r_{ij}} (\mathbf{r}_{\alpha\beta} + \phi_\beta \cdot \mathbf{S}_j - \phi_\alpha \cdot \mathbf{S}_i) \right) - \mathbf{C}_\alpha^{-1} \dot{\mathbf{C}}_\alpha \cdot \dot{\mathbf{S}}_i. \end{aligned} \quad (77)$$

Combining the two equations, we finally have

$$\begin{aligned} \ddot{\mathbf{S}}_i &+ \frac{1}{2} \phi_\alpha^{-1} \sum_\beta \sum_{i \neq j} \left(\frac{V'(r_{ij})}{r_{ij}} (\mathbf{r}_{\alpha\beta} + \phi_\beta \cdot \mathbf{S}_j - \phi_\alpha \cdot \mathbf{S}_i) \right) \\ &+ \mathbf{C}_\alpha^{-1} \dot{\mathbf{C}}_\alpha \cdot \dot{\mathbf{S}}_i + \phi_\alpha^{-1} \cdot \mathbf{b}_i = 0, \end{aligned} \quad (78)$$

where $i \in \alpha$. One may note that the second term in Eq. (78) contains both interaction of atoms within the α th cell and between two different cells, i.e., the case $i \in \alpha, j \in \beta$.

In summary, the dynamic equations of the proposed multiscale micromorphic molecular dynamics are as follows:

$$M_\alpha \ddot{\mathbf{r}}_\alpha = \sum_{\beta \neq \alpha} \sum_{i \in \alpha, j \in \beta} \mathbf{f}_{ij} + S_{\alpha 0} \bar{\mathbf{t}}_{\alpha 0} + \Omega_{\alpha 0} \bar{\mathbf{b}}_{\alpha 0}, \quad (79)$$

$$\ddot{\phi}_\alpha \cdot \mathbf{J}_\alpha^S = -(\mathcal{P}_\alpha^{int} - \mathcal{P}_\alpha^{ext}) \Omega_{\alpha 0} + \mathcal{M}_\alpha, \quad (80)$$

$$m_i \ddot{\mathbf{S}}_i = -m_i \mathbf{C}_\alpha^{-1} \cdot \dot{\mathbf{C}}_\alpha \cdot \dot{\mathbf{S}}_i + \phi_\alpha^{-1} \left(\sum_\beta \sum_{j \in \beta, j \neq i \in \alpha} \mathbf{f}_{ji} + \mathbf{b}_i \right), \quad (81)$$

where the mesoscale micromorphic deformation tensor is $\phi_\alpha = \mathbf{F}_\alpha \cdot \boldsymbol{\chi}_\alpha$. In Eqs. (79)–(81), one may see that there are two types of interaction conditions (boundary conditions) for each cell: (1) the cell-to-cell interactions and (2) the input of external forces through boundary. The first type of interaction is the internal interactions that are characterized by the terms

$$\sum_{\beta \neq \alpha} \sum_{i \in \alpha, j \in \beta} \mathbf{f}_{ij} \quad \text{and} \quad \mathbf{P}_\alpha^{\text{ext}} = \frac{1}{\Omega_{\alpha 0}} \sum_{\beta \neq \alpha} \sum_{i \in \alpha, j \in \beta} \mathbf{f}_{ij} \otimes \mathbf{S}_i,$$

where

$$\mathbf{f}_{ij} = \frac{V'(r_{ij})}{r_{ij}} (\mathbf{r}_{\alpha\beta} + \phi_\beta \cdot \mathbf{S}_j - \phi_\alpha \cdot \mathbf{S}_i). \quad (82)$$

The external force interaction are specified by the terms $S_{\alpha 0} \bar{\mathbf{t}}_{\alpha 0}$ and $\Omega \bar{\mathbf{b}}_{\alpha 0}$ in Eq. (79), and the term $\phi_\alpha^{-1} \mathbf{b}_i$ in Eq. (81).

Considering the following special case:

$$\mathbf{F}_\alpha = \mathbf{I}, \Rightarrow \phi_\alpha = \boldsymbol{\chi}_\alpha,$$

and $\mathbf{J}_\alpha^S = W_\alpha \mathbf{I}$, we recover the modified PR-MD,

$$W_\alpha \ddot{\boldsymbol{\chi}}_\alpha = -\boldsymbol{\chi}_\alpha \cdot (\mathcal{S}_\alpha^{\text{virial}} - \mathcal{S}_\alpha^{\text{ext}}) \Omega_{\alpha 0}, \quad (83)$$

$$m_i \ddot{\mathbf{S}}_i = -m_i \mathbf{C}_\alpha^{-1} \cdot \dot{\mathbf{C}}_\alpha \cdot \dot{\mathbf{S}}_i + \boldsymbol{\chi}_\alpha^{-1} \left(\sum_{j \neq i} \mathbf{f}_{ji} + \mathbf{b}_i \right), \quad (84)$$

where $\boldsymbol{\chi}_\alpha \mathcal{S}_\alpha^{\text{virial}} = \mathcal{P}_\alpha^{\text{int}}$ and $\boldsymbol{\chi}_\alpha \mathcal{S}_\alpha^{\text{ext}} = \mathcal{P}_\alpha^{\text{ext}}$ by comparing the two models.

IV. VALIDATION AND NUMERICAL EXAMPLE

To validate the proposed multiscale micromorphic molecular dynamics, in this section we employ it to study the phase transformation of nickel, which is also used as the validation case for PR-MD.²⁶ Different from Ref. 26, the following validation test is done in a finite size specimen without imposing periodic boundary condition. In our study, we focus on boundary effects and the non-equilibrium transition process of phase transformation.

Under uniaxial compression, the original FCC lattice of single crystal Nickel will go through structure change.^{22,23} The interaction between atoms is modeled by Morse potential, which is plotted in Fig. 5. It has the form of

$$\phi(r) = D(e^{-2\alpha(r-r_0)} - 2e^{-\alpha(r-r_0)}). \quad (85)$$

The interaction force is given by

$$F(r) = -\frac{\partial \phi(r)}{\partial r} = 2D\alpha(-e^{-2\alpha(r-r_0)} + e^{-\alpha(r-r_0)}). \quad (86)$$

With the constants $D = 3.5059 \times 10^{-20}$ J, $\alpha = 8.766/a_0$, and $r_0 = 0.71727 \text{ \AA}$. a_0 denotes the constants of the FCC lattice of nickel, i.e., $a_0 = 3.52 \text{ \AA}$,²⁶ with which the nickel single crystal will be in a global elastic energy minimum state for

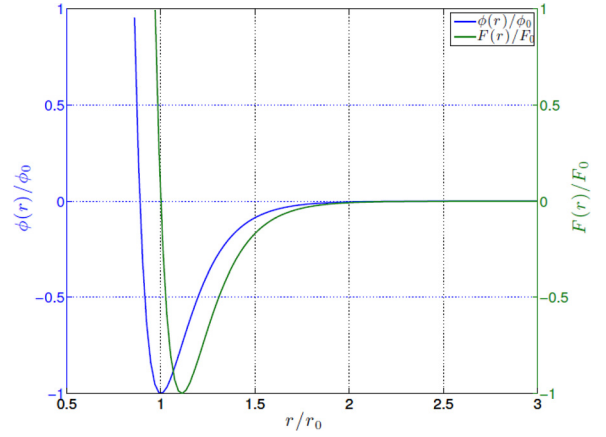


FIG. 5. Morse potential and the interatomic force.

bulk metal. Therefore, this is a stable equilibrium state, which is internal stress free. The atomic weight of nickel atom is 58.69 u.

During the entire simulation, the temperature is controlled at around 350 K by scaling microscale velocity on each cell every 10 micro time steps. Before the calculation, random perturbation of positions and velocities were assigned to ensure dynamics and the desired temperature. A 5000-step run in displacement-free state is conducted to obtain the optimal initial configuration. For demonstrative purpose, we let each micromorphic cell consisting of $3 \times 3 \times 3$ unit cells of Ni lattice, and the whole system has $3 \times 3 \times 3$ supercells as shown in Fig. 6. Among 27 supercells, there is one internal supercell which is not exposed to boundaries. We expect that it may be suitable to mimic the phase transformation as those in bulk metal. Thus, the whole model has in total 729 FCC unit cells and 2916 atoms according to basic crystallography.

We apply a compressive stretch

$$\mathbf{F} = \begin{bmatrix} 1 & 0 & 0 \\ 0 & \lambda & 0 \\ 0 & 0 & 1 \end{bmatrix},$$

on y direction, which is [010] direction in FCC lattice. The stretch is realized by moving the centers of mass of the top surface cells close to that of the bottom cells at each load step, and then allow a relaxation time so that the system can reach equilibrium. The compress-relax procedure gives a certain strain rate. Usually, we relax the system for 2000 steps for one incremental stretch of 0.03. During the loading process, the other components of \mathbf{F} may start to change according to Eq. (59), and we only control the principal stretch in y direction as a load parameter.

Fig. 7 shows the snapshots of loading history of the whole model (cross section) and the internal supercell (zoomed in). When the stretch is relatively small, i.e., $\lambda < 0.9$, the Ni bulk crystal went through somewhat elastic deformation. The particles are stretched uniformly. When the stretch increases, i.e., $\lambda < 0.8$, crystal slips were activated between the planes of {010} accompanied by the elastic in-plane deformation. The combined effect made the phase transition from original FCC lattice to HCP lattice happen.

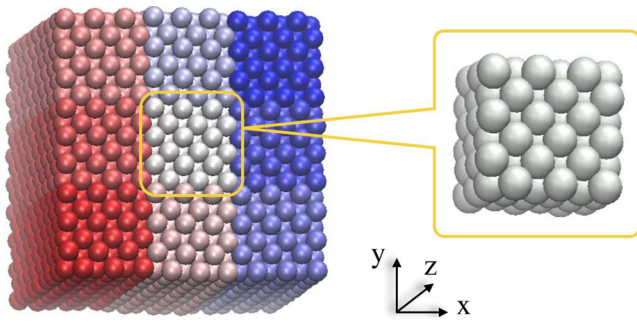


FIG. 6. The model setup: The system consists of $3 \times 3 \times 3$ supercells, and each supercell consists of $3 \times 3 \times 3$ unit cells.

During this process, the $\{001\}$ planes of FCC turned into $\{0001\}$ planes of HCP. We also noticed that the evolution of the whole structure is relatively smooth, no matter a cell is close to the boundary or in the interior of the simulation domain. This is the advantage of the proposed multiscale model over classic MD. Because if the displacements are prescribed on boundary atoms instead of supercells, the lattice pattern near the boundary will become irregular when those atoms are not free to seek the optimal positions. Whereas by prescribing displacements for the center of mass of boundary supercells as the boundary condition, it relaxes the constraint on each boundary atoms, and only the average displacements of the cell are controlled, i.e. that of the center of mass. This is essentially the macroscale boundary condition.

As we observe from the top in Fig. 8, the $\{010\}$ plane has a shape of parallelogram. This is due to the slip of adjacent planes of the $\{100\}$ type relative to each other. From

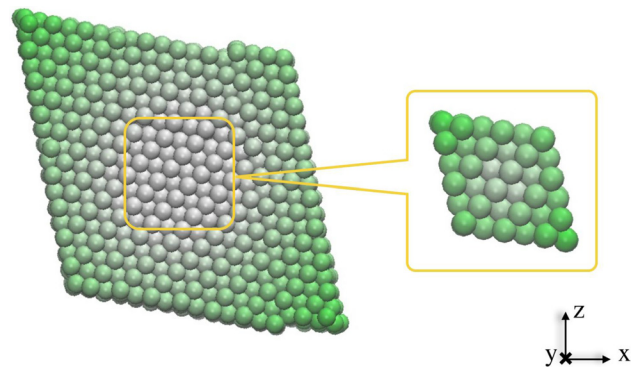


FIG. 8. The top view of final configuration when stretch $\lambda_y = 0.7$.

the figure, we find that the slips basically toward one direction, which formed regular pattern of parallelogram. However, this may not always be the case. Sometimes, the slips were influenced by imperfection of the initial structure and other factors, e.g., the relative slip between the fourth and the fifth planes on the right that is opposite to slips of other planes. They may be the result of initial perturbation of positions or velocity.

We have also studied the stress-strain relation for three different sizes of supercells, which have $3 \times 3 \times 3$, $4 \times 4 \times 4$, and $5 \times 5 \times 5$ unit cells, respectively (see Fig. 9). The data were obtained by averaging three runs for the same size of cells to reduce numerical error. We noticed that when the stretch is in the range of $[0.9 \ 1.0]$ and $[0.7 \ 0.75]$, the results have good agreement with the theoretical curve. When the stretch is in the range of $[0.75 \ 0.9]$, the points oscillate and

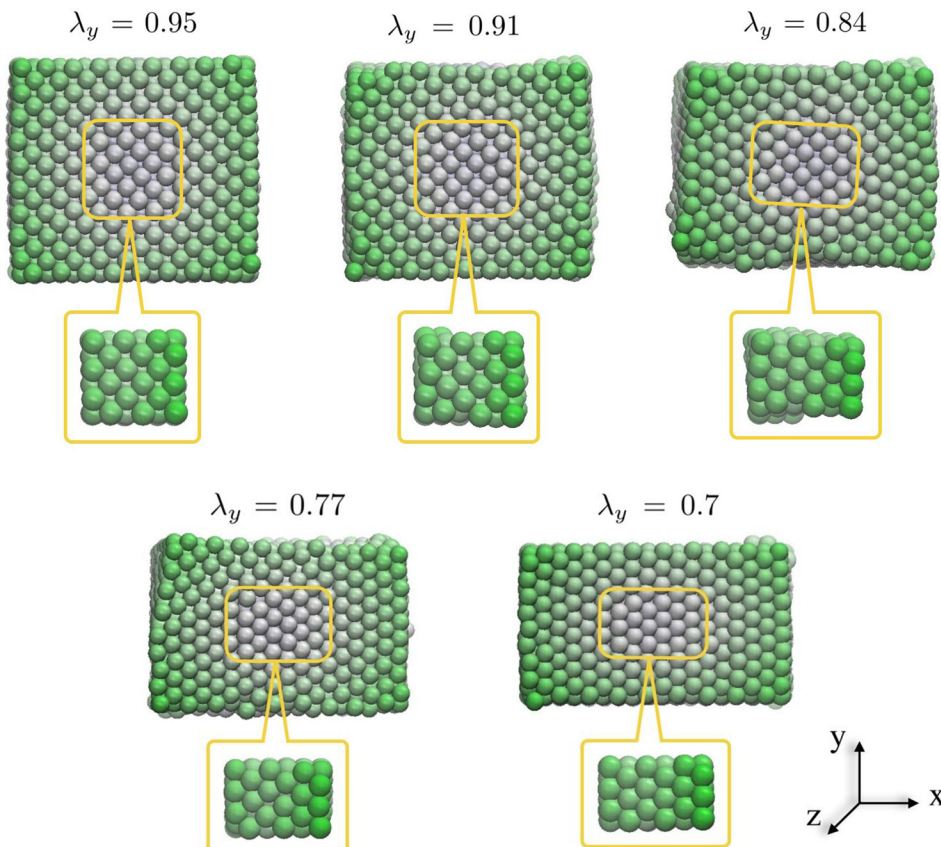


FIG. 7. Snapshots of the deformation history of the whole system and the internal cell.

large deviation is found for several points when comparing the theoretical curves. That is reasonable because [0.9 1.0] is the stable range for elastic deformation of FCC, and in the range of [0.7 0.75] of stretch, a stable HCP lattice is expected to form. When the stretch is in the range of [0.75 0.9], the lattice structure is not stable, and the stress varies from time to time. The phenomenon can be deduced from the energy landscape in Ref. 22. This study also shows that size of cells does not influence the result of regular deformation without defects (See Fig. 9). Further work on size dependency will be conducted when material defects are introduced.

V. DISCUSSIONS

Different from most multiscale methods proposed in recent years, the MMMD is not aimed at saving computation time or computer resource, but rather aimed at how to use first-principle based molecular dynamics to simulate macro-scale physical problems, and that is not a trivial task.

The conventional wisdom presumes that if we can simply increase the size of molecular dynamics ensemble we can simulate motions of macroscale objects by using first principle based molecular dynamics. In macroscale continuum mechanics or engineering mechanics, however, we hardly use the periodic boundary condition, nor do we impose boundary conditions on specific atoms at the boundary of the domain interested. In order to capture macroscale thermodynamics responses of a finite size atomistic ensemble system, we must be able to apply boundary conditions and initial conditions in continuum mechanics, and some other required constraint conditions to massive sized atomistic ensembles. This requires introducing macroscale thermodynamics measures that are related to microscale motions of atoms. In other words, the molecular system's multiscale characters must be carefully taken into account so that the microscale quantities can be correctly related to mesoscale and macroscale quantities based on first principle.

For example, in continuum mechanics, when we are solving macroscale mechanics boundary value problems, we need to impose boundary conditions that are either related to

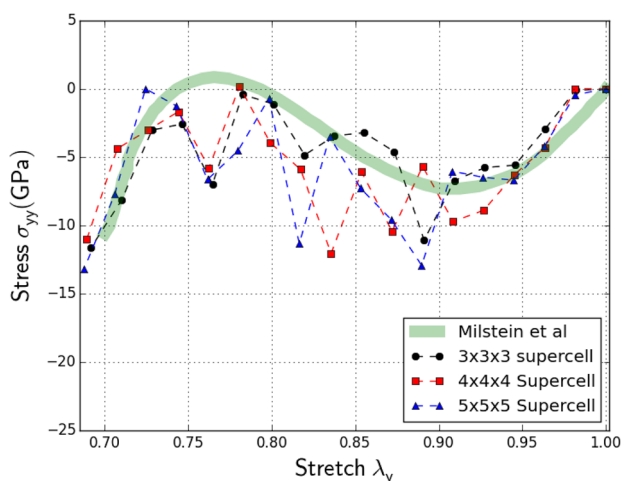


FIG. 9. Stress-strain relation under uniaxial displacement loading. Three different sizes of supercells are investigated. The curves are compared to the theoretical prediction by Milstein and Farber.²²

traction (stress) or displacements (strain) or some other macroscale thermodynamics variables such as temperature or electrical voltage. Hence, if we hope to use molecular dynamics to simulate the same macroscale problems based on first principle, we have to apply the same boundary conditions, which are consistent with macroscale measurements and practice, to first principle based molecular dynamics system. As computer and computing technology progress, the need for direct first principle molecular dynamics solution of macroscale problems will become more and more relevant, important, and urgent. Thus, we must develop a rigorous multiscale molecular dynamics that can couple macroscale thermodynamic variables with microscale statistical variables from first principle rather than from the direct coupling of molecular dynamics with phenomenological continuum mechanics by superficial boundary match or blending.

In this work, by utilizing the local equilibrium assumption, we repartition the first principle Lagrangian have extended the equilibrium (Andersen)-Parrinello-Rahman molecular dynamics to a non-equilibrium atomistic simulation, which can deal with finite size atomistic ensemble subjected to arbitrary macroscale boundary conditions. In doing so, we have proposed in the first time a novel concept of multiplicative multiscale decomposition that separates as well as couples macroscale continuum deformation with discrete atomistic motions.

By partitioning the Lagrange of the first-principle molecular dynamics ensemble, we have formulated a novel MMMD that can solve large scale molecular dynamics problems without the restriction of the periodic boundary condition and thermodynamics equilibrium condition. In other words, we can solve molecular dynamics problems in finite domains subjected macroscale boundary condition. The proposed multiscale micromorphic molecular dynamics reveals an intrinsic universal multiscale structure in molecular dynamics so that we can apply molecular dynamics to solve engineering problems with general thermodynamics conditions and arbitrary boundary conditions.

The MMMD formulation is essentially a global formulation of a set of local $N\mathcal{S}H$ ensembles. A future study is to extend the present theoretical formulation to other types of molecular dynamics ensembles such as local $N\mathcal{S}T$ ensemble. The computer implementation of the multiscale micromorphic molecular dynamics formulation will be reported in the second part of this work.

Last, the micromorphic molecular dynamics proposed in this work should be independent on the size of micromorphic cells as long as Eq. (31) holds. In fact, we have carried out numerical experiments on effect of the micromorphic cell size on MMMD simulation results (see Fig. 9). Depending on the actual size of the original problem, we would say, that the MMMD simulation results are almost independent from the micromorphic cell size in an range of several cubic nanometers to almost up to hundred cubic nanometers. We shall report the detailed study of size-effect in a separate paper. In fact, this range is also problem-dependent, because that once we get down to small scale, everything is size-dependent. If the micromorphic cell size is too small, it does not have enough atoms to provide correct statistical information; and

if the cell size is too large, one cannot capture locality of inhomogeneous field distributions such as abrupt change of stress and temperature distributions, or other size effects. As the fact of matter, this is a fundamental question that is at the heart of multiscale simulation, coarse grain theory, and statistical physics. One of the future works of this research is to systematically investigate this issue.

ACKNOWLEDGMENTS

Mr. Q. Tong was supported by a graduate fellowship from Chinese Scholar Council (CSC), and this support is greatly appreciated.

- ¹H. C. Andersen, *J. Chem. Phys.* **72**, 2384 (1980).
- ²Y. Chen and J. D. Lee, *Physica A* **322**, 359–376 (2003).
- ³Y. Chen and J. D. Lee, *Physica A* **322**, 377–392 (2003).
- ⁴Y. Chen, J. D. Lee, and A. Eskandarian, *Acta Mech.* **161**, 81–102 (2003).
- ⁵Y. Chen, *J. Chem. Phys.* **130**, 134706 (2009).
- ⁶F. Cleri, S. R. Phillpot, D. Wolf, and S. Yip, *J. Am. Ceram. Soc.* **81**, 503 (1998).
- ⁷F. Cleri, *Phys. Rev. B* **65**, 014107 (2001).
- ⁸A. C. Eringen, *Mechanics of Micromorphic Continua* (Springer, 1968).
- ⁹D. J. Evans and G. Morriss, *Statistical Mechanics of Nonequilibrium Liquids* (Cambridge University Press, 2008).
- ¹⁰J. Irving and J. G. Kirkwood, *J. Chem. Phys.* **18**, 817–829 (1950).
- ¹¹A. Laio and M. Parrinello, *Proc. Natl. Acad. Sci. U.S.A.* **99**, 12562–12566 (2002).
- ¹²A. W. Lees and S. F. Edwards, *J. Phys. C: Solid State Phys.* **5**, 1921 (1972).
- ¹³S. Li, X. Liu, A. Agrawal, and A. C. To, *Phys. Rev. B* **74**, 045418 (2006).
- ¹⁴S. Li and W. Liu, *Int. J. Numer. Methods Eng.* **45**, 251–288 (1999).
- ¹⁵S. Li, N. Sheng, and X. Liu, *Chem. Phys. Lett.* **451**, 293–300 (2008).
- ¹⁶S. Li and N. Sheng, *Int. J. Numer. Methods Eng.* **83**, 998–1038 (2010).
- ¹⁷X. Li, *Int. J. Numer. Methods Eng.* **83**, 986–997 (2010).
- ¹⁸X. Liu and S. Li, *J. Chem. Phys.* **126**, 124105 (2007).
- ¹⁹J. Marsden and T. J. R. Hughes, *Mathematical Foundations of Elasticity* (Prentice-Hall, Inc., 1983).
- ²⁰R. Martonák, A. Laio, and M. Parrinello, *Phys. Rev. Lett.* **90**, 075503 (2003).
- ²¹R. Martonák, D. Donadio, A. R. Oganov, and M. Parrinello, *Nature Mater.* **5**, 623–626 (2006).
- ²²F. Milstein and B. Farber, *Phys. Rev. Lett.* **44**, 277 (1980).
- ²³F. Milstein, *J. Appl. Phys.* **44**, 3825 (1973).
- ²⁴A. Murdoch, *J. Elasticity* **88**, 113–140 (2007).
- ²⁵M. Parrinello and A. Rahman, *Phys. Rev. Lett.* **45**, 1196 (1980).
- ²⁶M. Parrinello and A. Rahman, *J. Appl. Phys.* **52**, 7182 (1981).
- ²⁷P. Podio-Guidugli, *J. Elasticity* **100**, 145–153 (2010).
- ²⁸R. E. Rudd and J. Q. Broughton, *Phys. Rev. B* **58**, R5893 (1998).
- ²⁹R. E. Rudd and J. Q. Broughton, *Phys. Rev. B* **72**, 144104 (2005).
- ³⁰S. A. Silling, M. Epton, O. Weckner, J. Xu, and E. Askari, *J. Elasticity* **88**, 151–184 (2007).
- ³¹A. K. Subramaniyan and C. T. Sun, *Int. J. Solids Struct.* **45**, 4340–4346 (2008).
- ³²D. H. Tsai, *J. Chem. Phys.* **70**, 1375 (1979).
- ³³A. C. To and S. Li, *Phys. Rev. B* **72**, 035414 (2005).
- ³⁴Q. Tong and S. Li, “A Multiscale Molecular Dynamics for Representing Continuum Mechanical Loads,” *European Physics Letters* (submitted).
- ³⁵F. Vernerey, W. K. Liu, and B. Moran, *J. Mech. Phys. Solids* **55**, 2603–2651 (2007).
- ³⁶G. J. Wagner and W. K. Liu, *J. Comput. Phys.* **190**, 249 (2003).
- ³⁷M. Zhou, *Proc. R. Soc. London, Ser. A* **459**, 2347–2392 (2003).